Use of the dicarboxylate ligand *m*-phenylenedipropionate for the synthesis of new Mn/O clusters. Synthesis, characterization and magnetic properties

Cristina Cañada-Vilalta, John C. Huffman, William E. Streib, Ernest R. Davidson, George Christou *

Department of Chemistry and Molecular Structure Center, Indiana University, Bloomington, IN 47405-4001, USA

Abstract

The quest for new Mn clusters that display large spin ground states or that can serve as a synthetic model for the water oxidation center in PSII has been pursued by using the dicarboxylate ligand *m*-phenylenedipropionate (mpdp^{2-}). Ligand substitution of the acetate groups by this ligand in preformed clusters yields the compounds [Mn$_2$O(mpdp)(bpy)$_2$(MeCN)(H$_2$O)](ClO$_4$)$_2$ (**1**) and [Mn$_3$O(mpdp)$_3$(py)$_3$](ClO$_4$) (**2**), both similar in structure and properties to their acetate analogs. In a different reaction, mpdp^{2-} has allowed access to [Mn$_6$O$_7$(mpdp)$_3$(bpy)$_3$](ClO$_4$) (**3**), a new structural type whose electronic structure has been explored by measurements of its DC susceptibility and data indicate that it possesses a $S = 3/2$ ground state. © 2001 Elsevier Science Ltd. All rights reserved.

Keywords: *m*-Phenylenedipropionate; Dicarboxylate ligand; Mn/O clusters; Acetate analogs

1. Introduction

Our interest in Mn chemistry has developed from two main driving forces: (i) the search for new tetranuclear Mn systems that could serve as synthetic models of the water oxidation center responsible for the conversion of H$_2$O into O$_2$ in the photosystem II of the green plants and cyanobacteria [1,2]; and (ii) the quest for new compounds of diverse nuclearity that could display interesting magnetic properties, with a main focus on the large spin ground states and magnetic anisotropy that combined lead to single-molecule magnetism behavior [3]. Mn is an obvious choice from the biochemical point of view, but also from the magnetic perspective, since its redox and electronic properties allow it to exist in different oxidation states and show significant magnetic anisotropy at the Mn^{III} oxidation level. The ligand mpdpH$_2$ is a flexible dicarboxylate ligand in its deprotonated form, with similar properties

as traditional carboxylate units [4] but with the link between the two carboxylate groups adding a restriction that rules out some of the previously obtained Mn$_x$ structures.
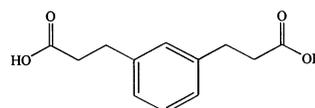
mpdpH$_2$

Our initial work with this ligand has led to the preparation of the compounds [Mn$_2$O(mpdp)(bpy)$_2$(MeCN)(H$_2$O)](ClO$_4$)$_2$ (**1**), [Mn$_3$O(mpdp)$_3$(py)$_3$](ClO$_4$) (**2**) and [Mn$_6$O$_7$(mpdp)$_3$(bpy)$_3$](ClO$_4$) (**3**), the latter with an unprecedented hexanuclear structure. The structures and properties of these species will be described.

2. Syntheses

Compounds **1** and **2** were obtained by ligand substitution of the acetate-containing clusters [Mn$_2$O(OAc)$_2$-

---

(bpy)$_2$(H$_2$O)$_2$](ClO$_4$)$_2$ and [Mn$_3$O(OAc)$_6$(py)$_3$](ClO$_4$), respectively, using the appropriate number of equivalents of mpdpH$_2$ in acetonitrile. In order to drive the reaction to completion, acetic acid was removed from the system by adding toluene and concentrating the solution by rotary evaporation; AcOH and toluene form an azeotrope (28% AcOH/72% toluene, b.p. 105° [5,6]). Complex **1** can also be synthesized by a direct reaction

between Mn(ClO$_4$)$_2$, bpy, mpdpH$_2$, N^{n}Bu$_4$ClO$_4$ and N^{n}Bu$_4$MnO$_4$ in acetonitrile, from which crystals are obtained after several hours. Compound **3** was obtained by oxidation of complex **1** with (N^{n}Bu$_4$)MnO$_4$ in acetonitrile, from which it crystallizes after 2–3 weeks. Complete details will be provided in the full paper [7].

3. Results and discussion

3.1. Description of the structures

3.1.1. [Mn$_2$O(mpdp)(bpy)$_2$(MeCN)(H$_2$O)](ClO$_4$)$_2$· 3MeCN (**1**)

An ORTEP representation of the cation of complex **1** is presented in Fig. 1. The cation unit consists of two hexacoordinated Mn^{III} atoms bridged by a μ-oxo group and two μ-carboxylate units from the ligand *m*-phenylenedipropionate. Each Mn ion is chelated by a bpy ligand, and the coordination sphere of each Mn center is completed by a different ligand; an acetonitrile and a water molecule, respectively. The latter is hydrogen-bonded to the two perchlorate anions that complete the structure (O(perchlorate)–O(water) distances of 2.77–2.86 Å) hence the unexpected asymmetry of the molecule; most of the similar dinuclear units reported in the literature contain only one type of terminal ligand [8,9]. The Mn ions exhibit a marked Jahn–Teller distortion, as expected for high spin d^4 Mn^{III} in near octahedral coordination. The distortion is significantly rhombic, with three statistically nonequivalent axes, the shortest one passing through the central μ-oxo bridge and the other two through carboxylate oxygen atoms.

The two bpy ligands are arranged in a quasi-perpendicular disposition. This is also the case for the longest axes of the two metal centers, the torsion angle O(H$_2$O)–Mn1–Mn2–N(MeCN) being 98.6°. This and other parameters are in the same range as those observed in analogous Mn^{III}μ-oxo and bis(μ-carboxylate) dinuclear complexes: these results underscore the great flexibility of the dicarboxylate ligand mpdp^{2-}, which is accommodated in the dinuclear unit without imposing any significant distortion.

3.1.2. [Mn$_3$O(mpdp)$_3$(py)$_3$](ClO$_4$) (**2**)

Complex **2** consists of three Mn^{III} ions in a triangular arrangement, connected by a central μ$_3$-oxide (Fig. 2). Two carboxylate groups from the same mpdp^{2-} ligand connect every pair of Mn ions, and the coordination is completed by a terminal pyridine ring on each metal. The structure does not possess any crystallographic element of symmetry: the three metals and their coordination spheres are approximately arranged around a C_3 axis, but the conformations of the three pyridine and the three dicarboxylate ligand rings are very different. The Mn–O distances and angles in each of the Mn ions
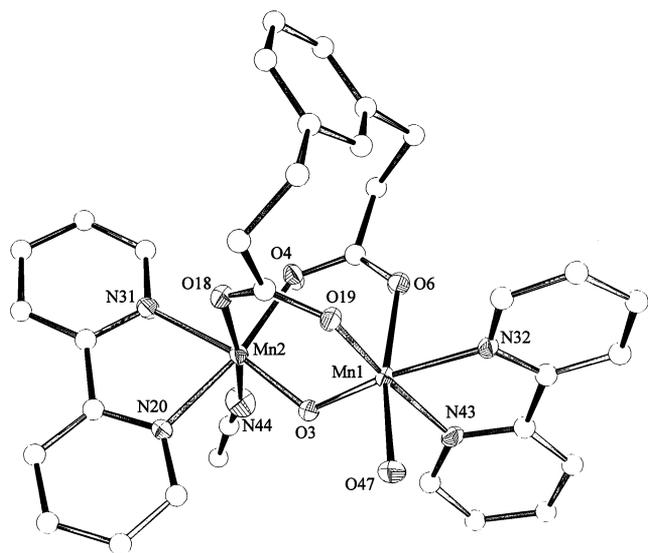

Fig. 1. ORTEP representation of the cation of **1**. Hydrogen atoms have been omitted for clarity, and carbon atoms are represented by spheres. The rest of the atoms are drawn at a 50% probability level.
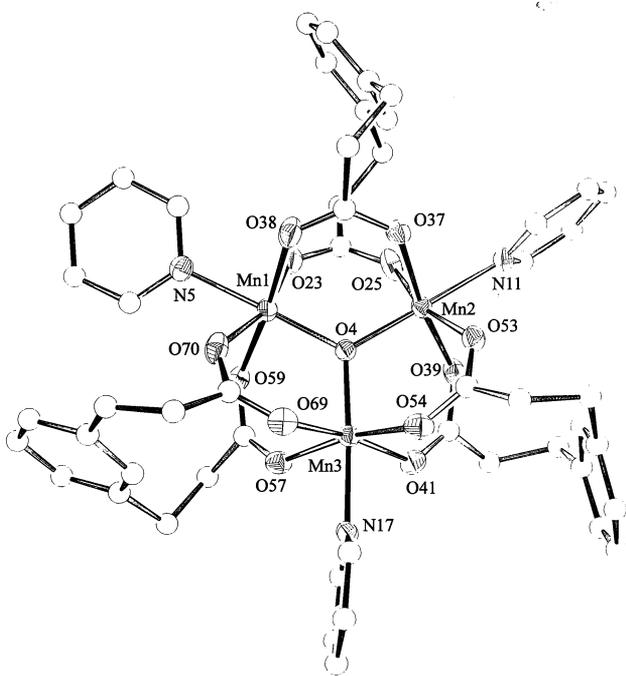

Fig. 2. ORTEP representation of the cation of **2**. Hydrogen atoms have been omitted for clarity, and carbon atoms are represented by spheres. The rest of the atoms are drawn at a 50% probability level.
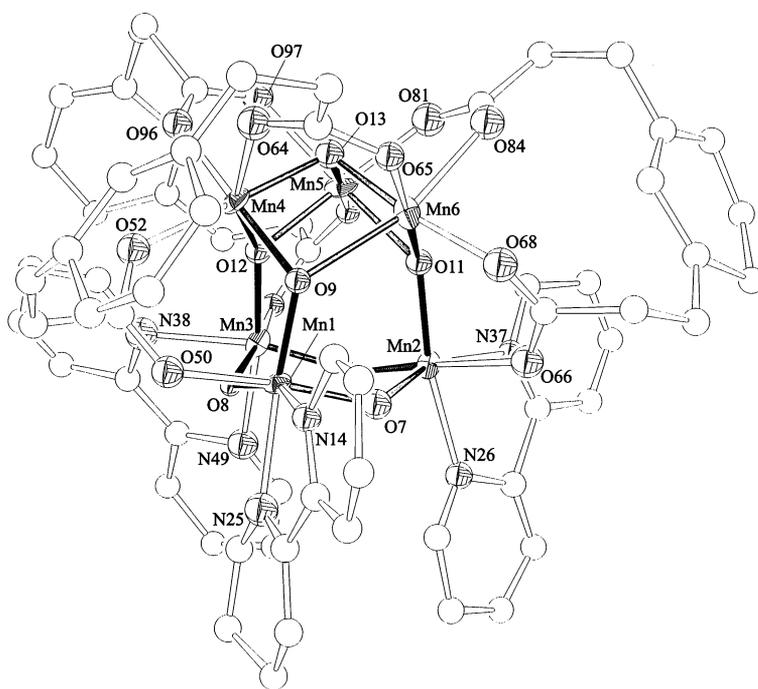
Fig. 3. ORTEP representation of one of the enantiomeric cations of compound **3**. Hydrogen atoms have been excluded and the rest of the atoms are drawn at a 50% probability level.

are also statistically nonequivalent, and therefore the structure can be appropriately described as a scalene triangle. The three Mn ions are Jahn–Teller distorted, with the longer axes going through oxides from the carboxylate groups. The structure is very similar to those observed for other $[Mn_3O]^{7+}$ complexes [10–12], emphasizing again that the flexibility of the dicarboxylate ligand allows it to adapt to many preexisting clusters without imposing any significant distortion.

3.1.3. $[Mn_6O_7(mpdp)_3(bpy)_3](ClO_4)·3.5MeCN$ (3)

An ORTEP representation of compound **3** is shown in Fig. 3. The core of the cation contains six Mn atoms disposed in a very distorted octahedral arrangement. The structure can be described as the superposition of two triangular units, with a non-crystallographic C_3 axis perpendicular to both and passing through O13. One triangular unit is a $[Mn_3^{IV}(\mu_2\text{-O})_3]^{+6}$ in which all Mn^{IV} atoms are hexacoordinated: Each of them is connected through two μ_2-oxides to the neighboring Mn^{IV} atoms from the same unit and through a μ_3-oxide to two Mn^{III} ions from the other trinuclear fragment. The three remaining coordination positions of the Mn^{IV} center in the first unit are occupied by two N atoms from a chelating bpy and by an O atom from a bridging carboxylate, which also binds to a Mn^{III} ion in the other triangle. The other fragment is an oxide-centered triangular $[Mn_3^{III}(\mu_3\text{-O})_4]^+$ unit. Each Mn^{III} is coordinated to three μ_3-O ligands, one being in the

center of the triangle and the other two in the edges, bridging this unit with the $[Mn_3^{IV}(\mu_2\text{-O})_3]^{+6}$ fragment. The other three coordination positions are occupied by bridging carboxylates: two of the bridges link the Mn^{III} with the other two Mn^{III} atoms in the same unit, whereas the third one connects the Mn^{III} center with a Mn^{IV} from the other triangle. Since the carboxylate ligand is formed by two propionate groups *meta*-substituting a benzene ring, the carboxylate bridges are connected: each Mn^{III}–OCO–Mn^{III} bridge is linked to a Mn^{III}–OCO–Mn^{IV} bridge.

The three Mn^{III}, high spin d^4 ions, present a clear Jahn–Teller distortion that causes one of the axes to be considerably longer then the other two, even though the ligands are the same for the three axes (a μ_3-O and a carboxylate). These Jahn–Teller elongated axes pass through one of the edge μ_3-oxide ions and the opposite carboxylate group, causing an apparent distortion in the $[Mn_3^{III}(\mu_3\text{-O})_4]^+$ unit, which would otherwise be hexagonal if both Mn and O atoms are taken into account. As an example, the distance Mn6···O9 is 2.209 Å, considerably larger than Mn6···O11, 1.849 Å.

3.2. Magnetism

3.2.1. $[Mn_2O(mpdp)(bpy)_2(MeCN)(H_2O)](ClO_4)_2·$ $3MeCN$ (1)

The variable temperature magnetic susceptibility of **1** was measured in the temperature range of 5–300 K.

The plot of the effective magnetic moment (μ_{eff}) vs. temperature per dinuclear unit is shown in Fig. 4: μ_{eff} decreases gradually with decreasing temperature from a value of 6.7 μ_{B} at 300 K (characteristic of two independent $S = 2$ metals) to 6.3 μ_{B} at 40 K, and then falls steeply to a value of 5.3 μ_{B} at 5 K. This is the magnetic behavior expected for a pair of weakly antiferromagnetically coupled high spin d^4 ions.

Owing to the extremely weak antiferromagnetic coupling, the behavior of the complex is very close to that of two non-interacting paramagnetic centers. The compound deviates from Curie behavior only at very low temperatures and this fact caused difficulty in the fitting of the experimental results to an appropriate theoretical expression. The exchange coupling J between the two metals is so weak that other effects that are usually neglected, such as intermolecular interactions or zero-field splitting (ZFS) of the excited states, become of the
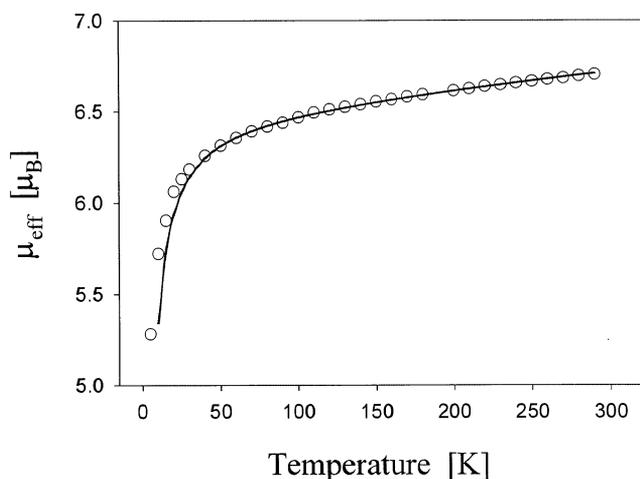

Fig. 4. Plot of the temperature dependence of the μ_{eff} for compound **1**. The solid line represents the least-squares fit to the data.
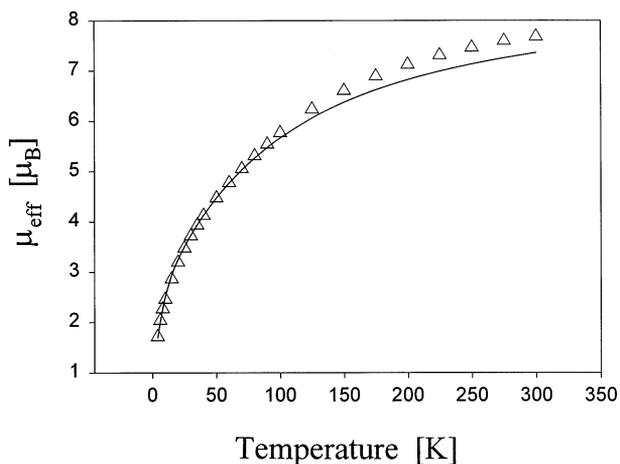

Fig. 5. Plot of the temperature dependence of μ_{eff} for compound **2** and least-squares fit (solid line) to the data for the global error minimum.

same order of magnitude. The best fit was found for the simplest model, assuming the spin Hamiltonian to be:

$$\hat{H} = -J_{12}\hat{S}_1\hat{S}_2$$

Least-squares fitting of the derived Van Vleck equation to the experimental data in the 50–290 K range afforded the following values: $g = 1.87$, $J = -0.58$ cm^{-1} and TIP $= 0.00149$ cm^3 mol^{-1}, where TIP is the temperature-independent paramagnetism. The theoretical curve is represented by a solid line in Fig. 5 (temperatures lower than 50 K have not been included in the fit but the plot does show the behavior predicted in that range).

While the values of g and J appear very reasonable, the TIP is about four times larger than what should be expected for a molecule with two high spin Mn$^{\mathrm{III}}$ (typically, a value of $\sim 4 \times 10^{-4}$ cm^3 mol^{-1}). The use of more complex equations including ZFS of the excited states or a correction (θ) to account for weak intermolecular interactions did not result in a lower value of the TIP. The reason for this is that, in all the cases, ZFS and intermolecular interactions were treated as a perturbation to the exchange interaction J, while, in this compound, all of these effects are comparable in value. A rigorous treatment should account for all of these factors, additionally including an anisotropic g parameter; the parameters to fit (J_{intra}, J_{inter}, D_1, D_2, g_{x}, g_{y}, g_{z}, TIP) would then be too many for the results to be reliable. The values obtained in the previous fitting are therefore not very accurate, but it seems safe to conclude that the coupling is antiferromagnetic and extremely weak (~ -0.5 cm^{-1}).

3.2.2. [Mn$_3$O(mpdp)$_3$(py)$_3$](ClO$_4$)·(**2**)

Measurements of the magnetic susceptibility of complex **2** were performed in the temperature range of 2.00–300 K. The plot of the μ_{eff} vs. temperature is shown in Fig. 5. The μ_{eff} at 300 K is 7.68 μ_{B}, slightly below the spin-only value associated with three non-interacting high spin Mn$^{\mathrm{III}}$ ions, namely 8.49 μ_{B}. It gradually decreases to 1.22 μ_{B} at 2.00 K, denoting the presence of antiferromagnetic interactions.

Structural considerations support the fitting of the data by the theoretical expression derived elsewhere [13,14] for an isosceles triangle, with two different values of intramolecular exchange interactions, J_{A} and J_{B}. Fitting of the experimental data to this model, together with a Weiss constant θ to account for the intermolecular interactions, yields two sets of values for which the error is minimum: $J_{\mathrm{A}} = -8.8(8)$ cm^{-1}, $J_{\mathrm{B}} = -6.2(6)$ cm^{-1} and $\theta = -3.2(4)$ K, and $J_{\mathrm{A}} = -6.0(7)$ cm^{-1}, $J_{\mathrm{B}} = -10(2)$ cm^{-1} and $\theta = -6(1)$ K. Each set of values corresponds to a different spin ground state, namely (0,2) and (1,1) using the format (S_{T}, S_{A}). The solid line in Fig. 5 corresponds to the first of these
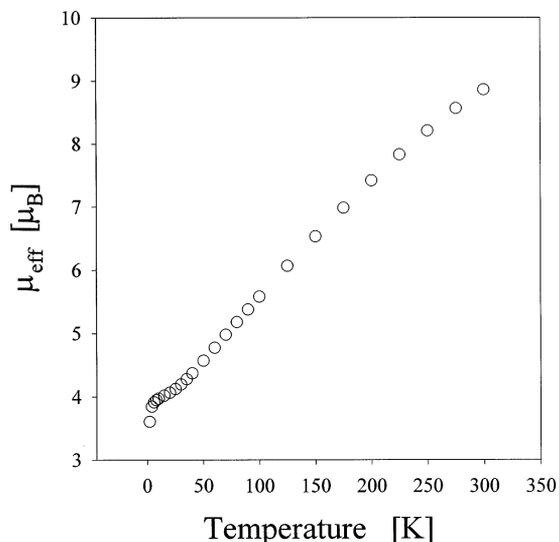
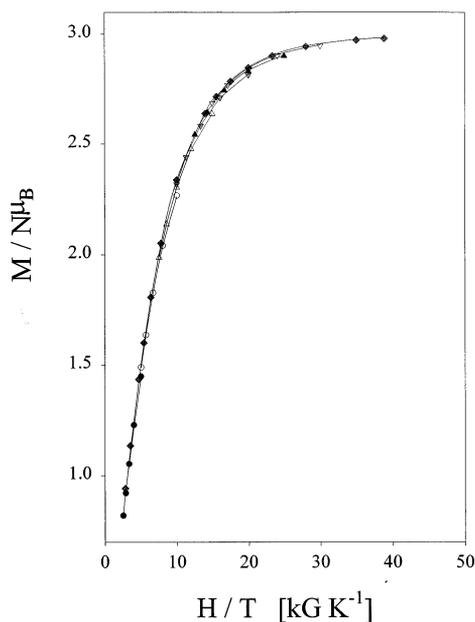Fig. 6. Dependence of the effective magnetic moment on the temperature in the 300–5 K range for complex **3**.

Fig. 7. Plot of reduced magnetization ($M/N\mu_B$) vs. H/T for complex **3**, where the symbol correspondence is as follows: $\blacklozenge$ = 7 T, $\triangledown$ = 6 T, $\blacktriangle$ = 5 T, $\blacktriangledown$ = 4 T, $\triangle$ = 3 T, $\bigcirc$ = 2 T, $\bullet$ = 1 T. The solid lines correspond to a fit of the data with fitting parameters given in the text.

minima. In both fittings, the triangular cluster possesses two antiferromagnetic exchange interactions of comparable magnitude that prevent (or *frustrate*) the preferred spin alignments. The result is therefore a compromise situation between the preferences of both forces and it depends largely on their relative magnitude. It is a classical example of spin frustration [15].

3.2.3. $[Mn_6O_7(mpdp)_3(bpy)_3](ClO_4)\cdot3.5MeCN$ (3)

The magnetic susceptibility of compound **2** was examined in the 5–300 K range. The μ_{eff} vs. temperature plot is shown in Fig. 6: it decreases gradually from 8.19 μ_B at 300 K to 4.03 μ_B at 30 K, where it almost plateaus, reaching 3.85μ_B at 5 K. This value is very close to 3.87 μ_B the spin-only value for a spin ground state of $S = 3/2$. The μ_{eff} value of 8.19 μ_B at 300 K is less than the 10.82 μ_B spin-only value ($g = 2$) expected for a $Mn_3^{III}Mn_3^{IV}$ complex with non-interacting metal centers. This suggests the presence of strong antiferromagnetic interactions within the molecule.

The complexity and low symmetry of the coupling system in **2** has precluded a fit of these data to obtain the exchange parameters. Even assuming idealized C_{3v} symmetry, four exchange parameters are required to describe the magnetic interactions between the six metal centers. The geometry is such that the equivalent operator approach cannot be applied and there are no reasonable approximations that could give a simpler coupling scheme. Therefore, it was not possible to quantify the different exchange interactions. However, valuable information can be obtained by other measurements.

To confirm the $S = 3/2$ ground state and to obtain the value of the ZFS parameter D, magnetization data were collected in the 1.80–25.0 K range with applied magnetic fields of 10–70 kG. A plot of the reduced magnetization $M/N\mu_B$ vs. H/T is given in Fig. 7. The expected saturation value for a $S = 3/2$ state with $g = 2.00$ is 3, which is just slightly above the values observed. These data were fit by diagonalization of the spin Hamiltonian matrix incorporating ZFS and Zeeman interactions and assuming only the ground state to be populated at these temperatures. Good fits (shown by solid lines in Fig. 7) were obtained with $S = 3/2$, $g = 2.01$ and $D = -0.79$ cm^{-1}.

4. Conclusions

Three new Mn clusters of nuclearities two, three and six have been obtained that contain the dicarboxylate ligand mpdpH$_2$ as well as oxo bridges and bpy or pyridine. The magnetic properties of these compounds have been investigated. Complex **1** displays a very weak antiferromagnetic coupling between the two Mn^{III} ions, and would be better described by a model that also considered the intermolecular interactions and ZFS at each metal center, since all of these contributions are of comparable magnitude. Compound **2** possesses three Mn atoms with antiferromagnetic coupling in an isosceles triangle disposition, which constitutes a typical example of spin frustration. Finally, complex **3** possesses an arrangement of six metal centers not observed previously; it is mixed-valent (3Mn^{III}, 3Mn^{IV}) and possesses

an $S = 3/2$ ground state. The combined results demonstrate the usefulness of mpdp^{2-} in Mn chemistry for the preparation of both analogs of known species and new structural types.

5. Supplementary material

Crystallographic data for the structural analysis have been deposited with the Cambridge Crystallographic Data Centre, CCDC Nos. 150674–150676 for compounds **1**–**3**, respectively. Copies of this information may be obtained free of charge from The Director, CCDC, 12 Union Road, Cambridge, CB2 1EZ, UK (fax +44-1223-336033; e-mail: deposit@ccdc. cam.ac.uk or www: http://www.ccdc.cam.ac.uk).

Acknowledgements

References

[1] V.K. Yachandra, K. Sauer, M. Klein, Chem. Rev. 96 (7) (1996) 2927.

[2] J. Limburg, V.A. Szalai, G.W. Brudvig, J.Chem. Soc., Dalton Trans. (1999) 1353.

[3] H.J. Eppley, S.M.J. Aubin, M.W. Wemple, D.M. Adams, H.-L. Tsai, V.A. Grillo, S. Castro, Z. Sun, K. Folting, J.C. Huffman, D.N. Hendrickson, G. Christou, Mol. Cryst. Liq. Cryst. 305 (1997) 167.

[4] R.H. Beer, W.B. Tolman, S.G. Bott, S.J. Lippard, Inorg. Chem. 30 (9) (1991) 2082.

[5] J.B. Vincent, H.R. Chang, K. Folting, J.C. Huffman, G. Christou, D.N. Hendrickson, J. Am. Chem. Soc. 109 (19) (1987) 5703.

[6] J.K. McCusker, H.G. Jang, S. Wang, G. Christou, D.N. Hendrickson, Inorg. Chem. 31 (10) (1992) 1874.

[7] C. Cañada-Vilalta, J.C. Huffman, W.E. Streib, E.R. Davidson, G. Christou, in preparation.

[8] J.B. Vincent, H.L. Tsai, A.G. Blackman, S. Wang, P.D.W. Boyd, K. Folting, J.C. Huffman, E.B. Lobkovsky, D.N. Hendrickson, G. Christou, J. Am. Chem. Soc. 115 (1993) 12353.

[9] J.E. Sheats, R.S. Czernuszewicz, G.C. Dismukes, A.L. Rheingold, V. Petrouleas, J. Stubbe, W.H. Armstrong, R.H. Beer, S.J. Lippard, J. Am. Chem. Soc. 109 (1987) 1435.

[10] J.B. Vincent, H.-R. Cheng, K. Folting, J.C. Huffman, G. Christou, D.N. Hendrickson, J. Am. Chem. Soc. 109 (1987) 5703.

[11] J. An, Z.-D. Chen, J. Bian, X.-L. Jin, S.-X. Wang, G.-X. Xu, Inorg. Chim. Acta 287 (1999) 82.

[12] J. Li, S. Yang, F. Zhang, Z. Tang, S. Ma, Q. Shi, Q. Wu, Z Huang, Inorg. Chim. Acta 294 (1999) 109.

[13] S.L. Castro, W.E. Streib, J.-S. Sun, G. Christou, Inorg. Chem. 35 (1996) 4462.

[14] G.B. Karet, S.L. Castro, K. Folting, J.C. Bollinger, R.A. Heintz, G. Christou, J. Chem. Soc., Dalton Trans. (1999) 67.

[15] O. Khan, Chem. Phys. Lett. 265 (1997) 109.